Journal of Materials Chemistry B

Accepted Manuscript

ROYAL SOCIETY OF CHEMISTRY

www.rsc.org/materialsB

Journal Name

ARTICLE

A Facile Construction of Gradient Micro-patterned OCP Coatings on Medical Titanium for High Throughput Evaluation of Biocompatibility

Received 00th January 20xx,
Accepted 00th January 20xx

DOI: 10.1039/x0xx00000x

www.rsc.org/

Ran Song,[a] Jianhe Liang,[a] Longxiang Lin,[a] Yanmei Zhang,[b,c] Yun Yang,[b,c] and Changjian Lin*[a,b,c]

Base on the superhydrophobic-superhydrophilic micro-patterned template, a facile construction of gradient micro-patterned octacalcium phosphate (OCP) coatings on titanium has been firstly developed for high-throughput evaluation of biocompatibility. The gradient OCP coatings with tunable crystal morphologies involving scattered-flower-like, scattered-flower-ribbon-like, short-ribbon-like and long ribbon-like had been fabricated in different micro-units on the same surface. The significant difference of mineralization behaviour of the gradient OCP coatings in the micropatterns was observed visually and efficiently. The in vitro cultures of MC3T3-E1 cell showed that the number and morphology of cells selectively adhered on the micro-units of gradient structure of OCP coatings were distinctly different, indicating that the cell is sensitive to the different structures of OCP coatings on medical titanium. The gradient micro-patterned constructions is hopeful to be a powerful method for not only high-throughput screening the biocompatibility of various biomaterials, but also efficient development of advanced biomaterials by controlling cell immobilization and inducing cell response.

1. Introduction

Surface chemistry, morphology and wettability play an important role in cell adhesion, proliferation and biological response[1-3]. Avoiding the disadvantages of conventional research methods, such as tedious process, consuming time, large amount of samples, cost and accidental error, micropatterned surface behaves an outstanding function in high-throughput investigation of the complex cell life behavior[4-11]. Superhydrophobicity with a water contact angle (CA) above 150° and superhydrophilicity with a CA below 5° are the two extreme cases of wettability and have attracted a great interest due to their importance in fundamental research and practical application[12, 13]. The differences of wettability can be used to engineer into the microtemplates with various sized micro-units of domains, which as a unique prospect of technique have been wildely applied in cell growth[14, 15], fluid microchips[16], microreactors[17, 18], and sensor arrays[19]. Among various applications, the micropatterning of living cells is attracting more and more attention because it can be used in broad range of researchs such as bioassays[20, 21], drugs[22], tissue engineering[23], and many fundamental studies of interaction between cells and materials[24-28]. Recent progress in micropatterning techniques has enabled the control of most of the crucial parameters of the cell microenvironment. Scopelliti et al. introduced novel methods for quantitative high-throughput characterization of protein-surface interaction, and indicated that the adsorption of proteins depended closely on the surface nanostructure and the relevant morphological parameter regulating the protein adsorption was nanometric pore shape[29]. Ito et al. investigated cells on the photo-immobilized protein micro-array and found that the adhesion behavior of cells relied on the kind of immobilized proteins and the kind of cells[30]. Thomson et al. developed a method of controlling Schwann cell placement and orientation in vitro by using microlithographically patterned laminin substrates[31]. Ye et al. proved an effective technique in controlling the shape and spreading of cells by a poly micropattern, and the square-shaped mouse osteoblast MC3T3-E1 cells were obtained in microwell arrays[7]. Tang et al. investigated both osteogenic and adipogenic differentiations of mesenchymal stem cells on a micropattern oil poly ethylene glycol (PEG) hydrogel, which was fairly linearly related to the extent of contact characterized by coordination number[32]. Shi et al. constructed a polydopamine (PDA)-coated parafilm with grooved micropatterns to induce the osteogenic differentiation of stem cells. They found that the adipose-derived mesenchymal stem cells cultured on the PDA-coated parafilm exhibited significantly higher osteogenic commitment in response to mechanical and spatial cues compared to the ones without stretch[33]. Yao et al. prepared an anion-exchangeable MgAl-layered double hydroxide (LDH) micropattern to act as both bioadhesive region for selective cell adhesion and nanocarrier for drug molecules to regulate cell behaviors[34]. Engineered micropatterns are able to provide a micrometer-scale, 3-

[a] State Key Laboratory for Physical Chemistry of Solid Surfaces, and Department of Chemistry, College of Chemistry and Chemical Engineering, Xiamen University, Xiamen 361005, China.
[b] Beijing Medical Implant Engineering Research Center, Beijing 100082, China.
[c] Beijing Engineering Laboratory of Functional Medical Materials and Devices, Beijing 100082, China.

dimensional and complex microenvironment for individual cells or for multi-cellular arrangements. The relationship of cell behaviors and micropatterned morphology, composition and structure can be detected and evaluated in a high-throughput way.

Titanium implants are extensively used for biomedical devices because of their favourable biocompatibility and mechanical properties, while osseointegration of them is limited since they are generally encapsulated by fibrous tissue after implantation[35-38]. Therefore, bioactive calcium phosphate (CaP) coatings or/and other chemical or biochemical modifications are frequently used to improve the bone integration properties[39]. Among them, octacalcium phosphate (OCP, $Ca_8H_2(PO_4)_6{\cdot}5H_2O$) is of particular interest in tissue mineralization biochemistry[40, 41], since it has been reported to be a direct precursor phase during the biomineralization process of bone and teeth[42, 43]. Previous work of our group demonstrted that a modification of thin OCP enhanced bioactivity of the roughened medical titainium[44]. Although OCP coatings with biocompatible structure becomes a hot field, very few researches forcusing on the relationship between different crystal morphologies of the OCP coatings with various micropatterns and their bioactivity have been reported[45, 46]. In this work, we emphasized to construct gradient OCP coatings with tunable crystal morphologies in various micropatterns on the same medical titanium surface to investigate the dependence of bioactivity and biocompatibility of OCP coatings on their crystal morphologies in a high-throughput way.

Plentiful methods of micropatterned surface have been developed, such as photolithography[47-50], ink-jet printing[51], soft lithograph[52-55] and micro-contact printing[56-61] . However, most of the conventional methods and new techniques can be only used for microfabrication on glass, silicon wafers or specific material, the materials chosen to be filled in the micro-patterns are also specific such as proteins, polymers, hydrogel and drug molecules, and costly equipements and rigorous fabrication conditions are generally required for the micropatterned fabrication. A facile, tunable and cheap microfabrication technique which is able to gain the gradient micropatterns on various functional materials is urgently needed. TiO_2 nanotube arrays films (TiO_2 NTAs) fabricated by electrochemically anodizing has been widely studied in various applications, such as biomaterials[62, 63], optoelectronics[64], photocatalysts[65, 66] and solar cells[67, 68]. Base on the precisely controllable ability of superhydrophilic-superhydrophobic properties on the TiO_2 nanotube arrays films, by surface assempling and photocatalysis[69-77], here we demonstrated a unique and advanced approach to fabricate gradient micro-patterned OCP coatings with biocompatible structure on medical titanium, which can be efficient and powerful to study the biocompatibility and cell-material interaction. As a micro-patterned material, the gradient micro-patterned OCP coatings has unique gradient function that can perform more effective high-throughput investigation for avoiding the disadvantages of conventional research methods, such as tedious process,

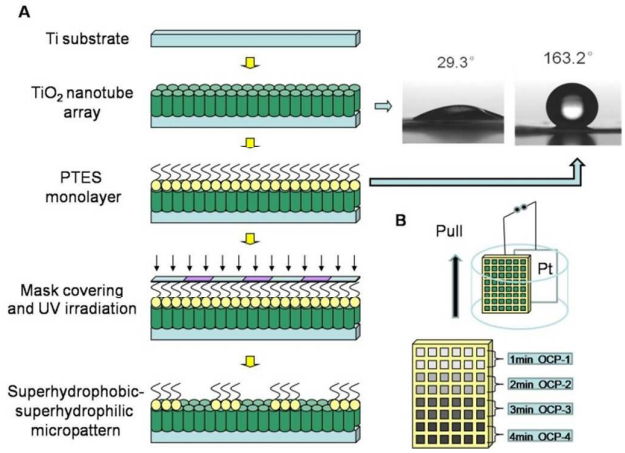

Fig. 1 Schematic outline of the preparation of superhydrophilic-superhydrophobic micro-patterned template based on molecular self-assembly and photocatalytic lithography（A）and then gradient OCP coatings on micro-patterned Ti substrate by pull-stop-pull electrodeposition (B).

consuming time, large amount of samples, cost and accidental error.

2. Experimental

2.1. TiO_2 micro-patterned templates.

Firstly, the TiO_2 NTAs was prepared by electrochemically anodizing on titanium sheets (purity 99.5%) in 0.5wt.% HF electrolyte with Pt counter electrode under 20V for 20min. Then the molecular assembling was conducted on the TiO_2 NTAs in a methanolic solution with 1% vol. 1H, 2H, 3H, 4H-perfluorooctyl-triethoxysilane (PETS, Degussa) for 1 h and then heated at 140℃ for 1 h to form a superhydrophobic film. Then, the sample surface was exposed to ultraviolet irradiation through a photomask with various sizes of micro-patterns for a decent period of time to selectively cleave the flouroalkyl chain. Finally, the TiO_2 microtemplates with superhydrophobic-superhydrophilic patterns were prepared[78].

2.2. Gradient electro-depositing of OCP.

The as-prepared superhydrophobic-superhydrophilic micro-patterns were used as a template for electrodepositing OCP on the superhydrophilic units only in an aqueous electrolyte containing 0.042mol/L $Ca(NO_3)_2$ and 0.025mol/L $NH_4H_2PO_4$ at pH 4.5 under galvanostatic mode to form OCP micro-patterns on titanium surface. And during the OCP electrodeposition, a pull-stop-pull method was used to control the sample to be moved out of the solution at a certain rate to enable gradient OCP coatings deposited on the different sized micro-patterns.

2.3. Simulated body fluid immersion test.

The bioactivity of the as-prepared gradient micro-patterned OCP coatings was examined from the biominalization in simulated body fluid (SBF). The samples with gradient OCP micro-patterns were immersed into SBF, which mimiced the composition of the inorganic part of human blood plasma. The SBF was prepared based on Kokubo's formulation by dissolving 8.035/L NaCl, 0.225g/L KCl, 0.355g/L $NaHCO_3$, 0.311g/L $MgCl_2 \cdot 6H_2O$, 0.292g/L $CaCl_2$ and 0.231g/L $KH_2PO_4 \cdot 3H_2O$ and 0.072g/L Na_2SO_4 into double distilled water buffered with tris-hydroxymethyl aminomethane to ph=7.3 at 37℃, and NaN_3 was added to inhibit the growth of bacteria. The samples were exposed to SBF under static conditions for 3 days for evaluating the transformation of OCP to hydroxyapatite (HA). The samples were thoroughly rinsed with double distilled water after immersion, and then air-dried for further examinations.

2.4. Surface characterization.

The surface morphologies and chemical compositions of the gradient micro-patterned OCP coatings and its mineralization products were characterized by a field emission scanning electron microscope (FE-SEM, Hitachi S4800, Japan) equipped with energy-dispersive X-ray spectroscopy (EDS, Inca system, Oxford Instruments, UK) and electron probe micro-analyzer (EPMA, JXA 8100, JEOL, Japan). The crystalline phases of the samples were identified by X-ray diffractometer (XRD, Rigaku Ultima IV, Japan) with Cu-Ka radiation source at 35 kV and 15 mA. Three-dimensional profile images on surface were measured using a 3D Optical Surface Metrology System (DCM 3D, Leica Microsystems, Germany).

2.5. Cell culture.

Mouse MC3T3-E1 preosteoblastic cells were used for all biological assays. The MC3T3-E1 cells were cultured in the medium contained alpha-minimum essential medium(α-MEM) supplemented with 10% FBS, 100 units/mL penicillin, and 100 μg/mL streptomycin and maintained under a humidified atmosphere with 5% CO_2 at 37 °C. The cells were detached from the culture dish when 90% confluented with 0.25% trypsin, centrifuged at 1000 rpm for 5 min, and resuspended in fresh culture medium. Four groups of samples (gradient micro-patterned OCP coatings, circle with diameter 100 μm and gap length 100μm) were sterilized by soaking in 75% alcohol for 1 h, air-dried and wetted with phosphate buffer saline (PBS). Then the samples were placed into a 6-well plate and seeded with cells at a density of 5×10^4 cells/cm^2.

2.6. Cell adhesion and morphology.

After incubating for 6 h and 24 h, all groups of the samples were rinsed with PBS to remove the nonadherent cells.

The group 1 of cells were stained by 3,6-bis (dimethylamino) acridine zinc chloride hydrochloride (Acridine Orange, Sigma, USA) and photographed under a fluorescence microscope (Nikon Ti–U, Japan).

The group 2 of cells were fixed with 4% paraformaldehyde (PFA) for 2 h, stained by 4′ -6′ -diamidino-2-phenylindole (DAPI, Sigma, USA), then photographed under a fluorescence microscope and counted. All of the data were collected from at least three samples for each group and expressed as mean values ±standard deviations. A value of $p< 0.05$ was considered to be statistically significant.

The group 3 of cells were fixed with 2.5% glutaraldehyde for 20 min, stained with Phalloidin-Tetramethylrhodamine B isothiocyanate (Phalloidin-TRITC, Sigma, USA) at room temperature in darkness for 1 h and further stained with DAPI for 5 min, then photographed under a laser confocal fluorescence microscopy (LSCFM, TCS SP5, Leica Microsystems, Germany).

The group 4 of cells were fixed with 2.5% glutaraldehyde for 2h, and dehydrated in graded concentrations of ethanol (30, 50, 70, 90, and 100%). Afterward, the samples were dried in a freeze-dryer (Eyela FDU-1200, Tokyo Rikakikai, Japan), sputtered with a thin platinum layer, and then examined by SEM observations.

3. Results and discussion

3.1. Fabrication of gradient micro-patterned OCP.

The fabrication of the superhydrophobic-superhydrophilic micro-patterns on TiO_2 NTAs films using photocatalytic lithography is shown in the schematic outline in Fig 1 (A). A facile method was designd to fabricate gradient micro-patterned OCP coatings with biocompatible structure on medical titanium. Because of the extrame difference of wettability between the micro-units and their the gaps on the superhydrophobic-superhydrophilic micro-patterned template, the aqueous electrolyte contacted well and the OCP crystals were preferentially deposited on the superhydrophilic units,

while the superhydrophilic locations with air trapped at the liquid/solid interface were prevent from the contact of electrolyte. Therefore, electrodeposition process can only take place in the superhydrophilic regions. Different deposition conditions such as deposition current density and deposition time can be controlled to fabricate gradient micro-patterned OCP coatings with various morphologies and other structured

CaP as well. The patterns with different shape and size can be realized by using various designed photomasks.

The fabrication procedure of gradient OCP coatings on the micro-patterned Ti substrate is schematically shown in Fig 1 (B). The Ti sheets with superhydrophobic-superhydrophilic micro-patterned template were immersed in the aqueous electrolyte containing 0.042mol/L $Ca(NO_3)_2$ and 0.025mol/L $NH_4H_2PO_4$ at pH 4.5. And a galvanostatic mode of 0.5mA/cm^2 was supplied with Pt sheet as counter electrode to deposited OCP film in the micro-patterns on titanium surface for 1min. Then the sample was quickly pulled out from the solution for a distance of 2mm while keeping electrodeposition for another 1min, then again the sample was quickly pulled out from the solution for

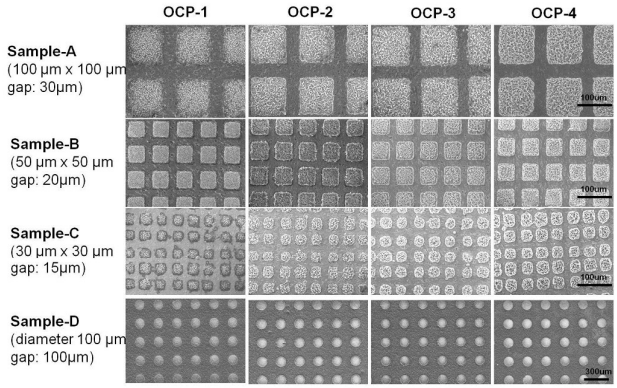

Fig. 2 SEM images of the gradient micro-patterned OCP coatings on superhydrophobic-superhydrophilic micro-patterned templates with different dimensions and structures on four samples(A,B,C,D): OCP-1 (1 min) ; OCP-2 (2 min) ; OCP-3 (3 min) ; OCP-4 (4 min) .

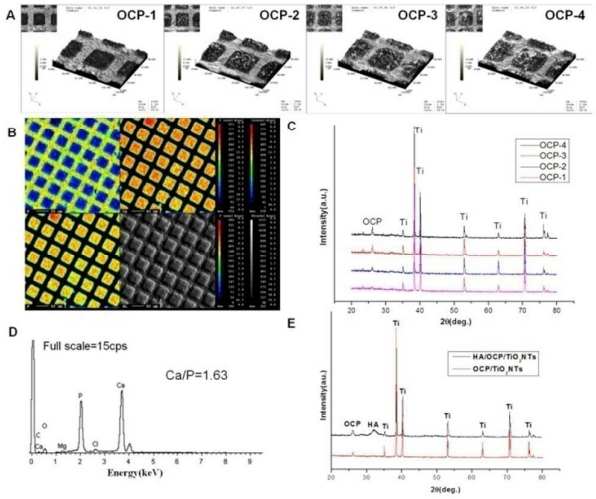

Fig. 3 3D profile images of the gradient micro-patterned OCP coatings (A); Element distribution of the micro-patterned OCP coatings (B); XRD spectra of the gradient micro-patterned OCP coatings (C); EDS spectra of the bone-like apatite formed on the micro-patternd OCP coatings after soaking in SBF for 3 days (D); XRD spectra of the patterned OCP coatings and the micro-patterned OCP coatings after soaking in SBF for 3 days (E).

another distance of 2mm while keeping electrodeposition for another 1min ……., By such multiple procedure of pull-stop-pull electrodepositing of OCP, the gradient micro-patterned OCP coatings were obtained as shown in Fig 2, where the images of OCP-1, OCP-2, OCP-3 and OCP-4 indicated four locations of micro-patterned OCP on the same surface by electrodeposition for 1, 2, 3, 4 min respectively. Therefore, the nucleation and growth of OCP crystal can be controlled on the different locations on the same surface to finally form a gradient micro-patterned OCP coatings by adjusting of electrodepositing conditions such as depositing time and current density.

3.2. Strucure dependence of micro-patterned OCP on fabrication.

The 3D profile images of the gradient micro-patterned OCP coatings are exhibited in Fig 3 (A). The typical topography of the micro-patterned OCP coatings with nano-structure was orderly and uniform in three dimensions. There was an obvious increase in the thickness of the OCP coatings from OCP-1 to OCP-4 because of the increasing deposition time.

The EPMA images in Fig 3 (B) reflect the element distribution on micro-patterned OCP coatings visually. Elements of Ca and P (corresponded to OCP) showed significantly large amount in the superhydrophilic micro-units while F (corresponded to PTES) behaved the opposite. It indicated that almost removal and photodecomposition of fluoroalkyl chain took place in the micro-units under ultraviolet illumination, which led to the electrodeposition of OCP only at the superhydrophilic micro-units with distinct boundaries.

The XRD measurement shown in Fig 3 (C) confirms the presence of OCP with characteristic diffraction line to (002) plane at 26° (JCPDS # 44-778), while other reflections were ascribed to the TiO2 /Ti substrate. As was seen in the spectra, the intensity of the (002) peak of OCP was enhanced with the increasing deposition time. The sharp diffraction peaks indicated a well developed crystalline structure and a preferred crystal orientation with respect to the c-axis perpendicular to substrate. The quantity of OCP crystal kept increasing with the increasing deposition time since the intensity of a XRD peak was proportional to the quantity of a substance theoretically, which was also obviously displayed in the 3D proflie images of the gradient micro-patterned OCP coatings.

3.3. Evaluation of mineralization ability.

Fig.4 (A) shows the SEM images of the prepared gradient OCP coatings with different crystal morphologies changing from scattered-flower-like, scattered-flower-short-ribbon-like, short-ribbon-like, and long ribbon-like, due to the different time of electrodeposition. The test of SBF was adapted to evaluate the mineralization ability and in vitro bioactivity of OCP coatings with various morphologies in the same physiological conditions[79]. It was found that the different morphologies of OCP crystals behaved significantly different ability of mineralization for 3 days soaking in SBF solution, as shown in Fig 4 (B). The scattered-flower-like morphology of the OCP crystals (OCP-1) almostly maintained while very few of some new CaP precipitates were visible on the surface of the original morphology of the OCP crystals (OCP-1), and much more CaP precipitates were observed on the scattered-flower-short-ribbon-like OCP crystals (OCP-2). Further more, the villus-like precipitates almost covered the short-ribbon-like and long-ribbon-like morphologies of the OCP crystals (OCP-3, OCP-4). The newly formed CaP layer on OCP coatings showed a similar morphology to that of natural bone. The EDS spectra of the CaP precipitates formed on the micro-patternd OCP coatings after incubation in SBF for 3 days was shown in Fig 3

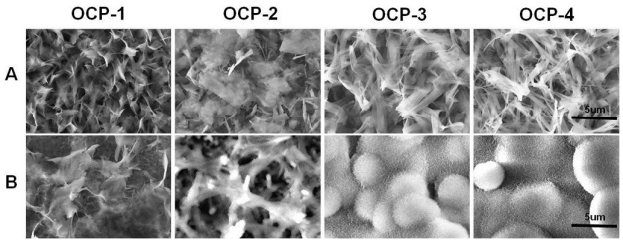

Fig. 4 SEM images of the gradient micro-patterned OCP coatings with different dimensions and structures: morphologies with a higher magnifacation of corresponding images of sample A in Fig 2 (A) ; CaP precipitates on the different locations of micro-patterned OCP coatings after soaking in SBF for 3 days(B).

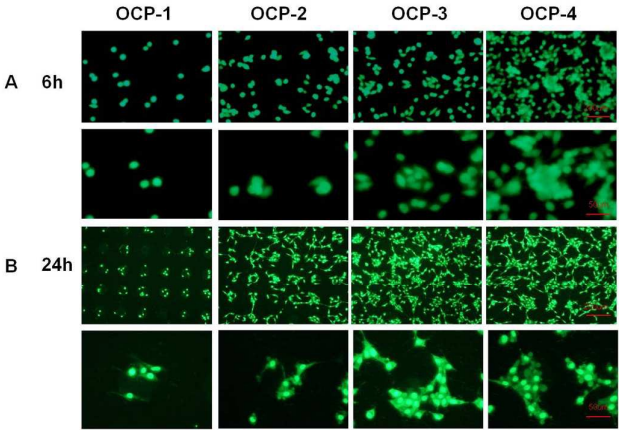

Fig. 5 Fluorescence images of MC3T3-E1 cells cultured on the the gradient micro-patterned OCP coatings stained with Acridine Orange: 6h(A); 24h(B).

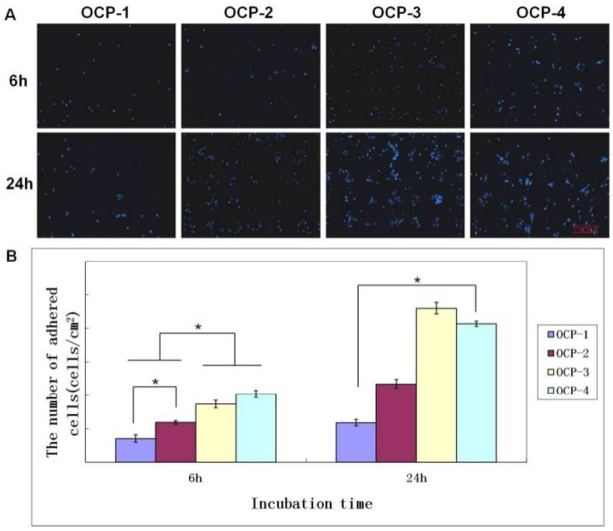

Fig. 6 Fluorescence images of MC3T3-E1 cells cultured on the the gradient micro-patterned OCP coatings stained with DAPI after incubation for 6h and 24h (A); the quantitative results of cell numbers. Significance: *, $p<0.05$ (B).

(D), indicating the presence of calcium and phosphorus as well as small amounts of sodium and magnesium. The Ca/P atomic ratio of the precipitates newly formed was 1.63, which was similar to that of HA phase. The XRD spectra of the micro-patterned OCP coating after incubation in SBF for 3 days was shown in Fig 3 (E). After soaked in SBF for 3 days, the (002) reflection of OCP was still obtained and even dominant, indicating the crystal growth retained a preferred c-axis orientation during immersion in SBF. The mineral crystals in nature bone had a similar preferred orientation. Several gentle peaks appeared at 32-34° , which were consistent with the standard XRD peaks for HA (JCPDS # 9-432). It implied that, after soaked in SBF for 3 days, the main phase on the OCP coatings evolved from OCP toward an apatite phase and the orientation of the newly formed apatite resulted from the similar structure of the prepared coatings. The significantly different mineralization behaviour of the gradient OCP coatings was demonstrated visually in the micro-patterns on the same surface of sample, which was an advanced evaluation with high efficiency and may aviod from accidental error occured among different samples and surroundings at the same time. The ability and bioactivity of OCP-4 was relatively higher among the four, which proved that the surface composition, thickness and structure of the prepared coatings play a crucial role in the process of apatite formation in body environment[80].

3.4. Assessment of cell responses.

The fluorescence images of MC3T3-E1 cells cultured on the same gradient micro-patterned OCP coatings stained by Acridine Orange and DAPI respectively are shown in Fig 5 and Fig 6 (A), and the quantitative results of cell numbers are listed in Fig 6 (B). After 6 h incubation, MC3T3-E1 cells adhered almost onto the superhydrophilic micro-units and formed cell patterns on the OCP coatings, due to the different wettability between micro-units and gaps, and different biocompatibility of OCP micropatterns as well. Moreover, some important proteins involved in cellular adhesion and proliferation, such as fibronectin and vitronectin, which may preserve an active conformation on superhydrophilic regions rather than on superhydrophobic surface[81, 82]. The number of cells adhered onto the gradient OCP coatings was markedly different depending on the structures of OCP deposited for different times, only 1-2 cells in one unit of OCP-1 electrodeposited for 1 min, 2-3 cells in one unit of OCP-2 prepared for 2 min, 2-6 cells in one unit of 3 min precipitated OCP-3, and 5-10 cells in one unit of OCP-4 deposited for 4min. According to the quantitative analysis shown in Fig.6 (B), the cells number adhered on the micropatterned units increased with the OCP thickness (prepared for different times) after 6 h culture. After 24 h incubation, the cells adhered onto the superhydrophilic micro-units of OCP were well-spread and began to proliferate. The number of cells adhered onto the different OCP coatings behaved different degree of the growth, which appeared to be

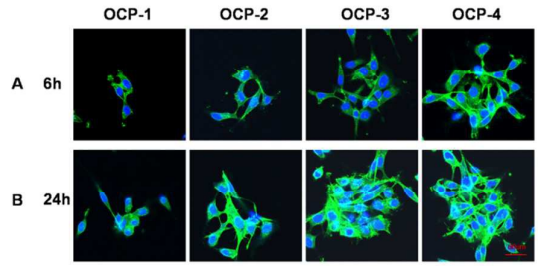

Fig. 7 Fluorescence images of MC3T3-E1 cells cultured on the the gradient micro-patterned OCP coatings cytoskeletal actin staining with Phalloidin-TRITC (green) and nuclei staining with DAPI (blue): 6h(A); 24h(B).

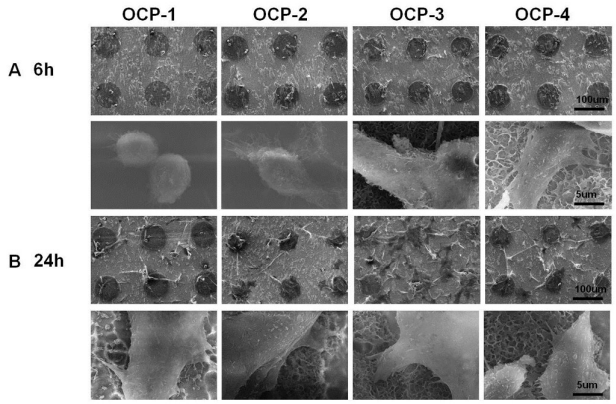

Fig. 8 SEM images of of MC3T3-E1 cells cultured on the the gradient micro- patterned OCP coatings: 6h(A); 24h(B).

higher by 67% on OCP-1, 98% on OCP-2, 166% on OCP-3, and 103% on OCP-4 respectively than that incubated for 6 h.

Cell adhesion, spreading activity and mobilization of cells attached on the different OCP units after 6 h and 24 h of incubation are assayed by staining with TRITC and DAPI to visualize the F-actin and nuclei respectively[83, 84]. The results are shown in Fig 7, while Fig 8 provides cell morphologies by SEM observations. It is indicated that the spreading of cells was remarkably regulated by the different OCP coatings during the 6 h incubation, The cells adhered with a sphere or fusiform shape onto the micro-units of OCP-1, less bioactive because of too thin for OCP coatings. And the cells spreaded out with a fusiform shape on OCP-2, a small amount of filopodia was stretched out. In contrast, the cells on the OCP-3 micro-units displayed a polygonal shape, while cells on OCP-4 spreaded much better with a polygonal shape and prominent filopodia and lamellipodia protrusions[85, 86]. The expression of F-actin on OCP-4 was significantly better than that on OCP-1, OCP-2 and OCP-3. After 24 h incubation, most cells were well-spreaded and began to proliferate, with a long fusiform shape on the micro-units with OCP-1 and with an polygonal shape on the OCP-2, most cell body on the micro-units and a little prominent filopodia on the superhydrophobic gaps. Apart from the difference in the number of cells adhered onto the different OCP coatings, the spread of cells behaved remarkably different, implying that the different bioactivity was closely depended on the structures of OCP coatings in the micro-units. Cells spreaded out crowdedly and actively on the micro-units with OCP-3 and much more obviously on OCP-4 with extense polygonal shape and a large amount of prominent filopodia and lamellipodia protrusions, cell podia bridging over in the single micro-units and among different micro-units. A few cells adhered onto the superhydrophobic gaps with low viabiliy because of the space limitation. The expression of F-actin on OCP-2, OCP-3 and OCP-4 was better than that on OCP-1. Mobilization of cells can be indicated in the fluorescence and SEM images,too. Toward OCP micro-units with gradient coatings, cells tended to adhere to the border of the micro-units in the initial adhesion and spreaded out to the inner part of the micro-units until the units were fully occupied and then had to spread out of the micro-units.

During the initial adhesion, the coatings of OCP-4 behaved the best bioactivity with most cell adhesion and active cell spreading. It was found, after incubation for 24 hours, that the coatings of OCP-3 was able to modulate the cells to be more stereoscopic with the fastest proliferation, indicating a more superior of bioactivity comparing with OCP coating in micro-units. As a result, the composition, thickness and structure of the OCP coating play a crucial role in the adhesion, spreading, and proliferation of mouse MC3T3-E1 cells.

All in vitro tests of MC3T3-E1 cell demonstrated that the cells showed different number and morphology adhered on the different micro-units in which cells were effectively limited, indicating that the cells are of high sensitivity to the gradient structure of OCP coatings, and the gradient micro-patterns of biomaterials can be as a powerful tool for not only high throughput evaluation of biocompatibility and bioactivity, but also highly efficient design and construction of various advanced biosurfaces.

Conclusions

In summary, we have successfully developed an approach for fabricating biocompatible gradient micro-patterned OCP coatings based on superhydrophobic-superhydrophilic micro-patterned template. The patterned OCP coatings with different morphologies behaved significantly different ability of mineralization in SBF and bioactivity in the adhesion, spreading and proliferation of mouse MC3T3-E1 cells. The equipements we used in our approach are very simple and can be easily performanced in general laboratory conditions. In our approach, the substrate material can be titanium or other metallic materials, and various biomaterials such as calcium phosphate, proteins, antibacterial agents etc. can be deposited to the superhydrophilic-superhydrophobic micro-patterned templates by the wet chemical methods to fabricate functional gradient micro-patterned coatings. The gradient micro-

patterned OCP coatings discribed in this manuscript was just an example of the construction of gradient micro-patterned coatings. Because titanium is a wildly-used biomaterials and also electrical conductor, electrochemical method can be used to deposit various biofilms on the superhydrophilic-superhydrophobic micro-patterned templates in more accurate and controllable mode. It can become a facile and efficient technique for fabrication of various gradient and micro-patterned functional materials by using the strategy of superhydrophobic-superhydrophilic micro-patterned template and pull-stop-pull approach. Meanwhile, the bioactive micro-patterns with gradient coating is of an effective modulation for spatially control of dynamic cells attachment and proliferation, which is enable high throughput evaluation of the cell behaviors, interaction of cell and materials, and bioproperties in a single experiment. The development of gradient micro-patterns is promising for not only high throughput evaluation of biocompatibility and bioactivity, but also highly efficient design and construction of various functional materials.

Acknowledgements

The authors thank the financial supports from the the Natural Science Foundation of China (51571169 and 21321062), and International Cooperation Program of China (2014DFG52350).

*Correspondence - cjlin@xmu.edu.cn

Notes and references

1. J. Y. Wong, J. B. Leach and X. Q. Brown, *Surface Science*, 2004, **570**, 119-133.
2. C. Chai and K. W. Leong, *Mol. Ther.*, 2007, **15**, 467-480.
3. D. E. Discher, P. Janmey and Y. L. Wang, *Science*, 2005, **310**, 1139-1143.
4. D. Guarnieri, A. De Capua, M. Ventre, A. Borzacchiello, C. Pedone, D. Marasco, M. Ruvo and P. A. Netti, *Acta Biomaterialia*, 2010, **6**, 2532-2539.
5. P. Costa, J. E. Gautrot and J. T. Connelly, *Acta Biomaterialia*, 2014, **10**, 2415-2422.
6. B. Cao, Z. H. Li, R. Peng and J. D. Ding, *Biomaterials*, 2015, **64**, 21-32.
7. F. Ye, B. H. Ma, J. Gao, L. Xie, C. Wei and J. Jiang, *Journal of Biomedical Materials Research Part B-Applied Biomaterials*, 2015, **103**, 1375-1380.
8. M. Thery, *Journal of Cell Science*, 2010, **123**, 4201-4213.
9. Y. Nahmias and D. J. Odde, *Nature Protocols*, 2006, **1**, 2288-2296.
10. M. S. Hahn, L. J. Taite, J. J. Moon, M. C. Rowland, K. A. Ruffino and J. L. West, *Biomaterials*, 2006, **27**, 2519-2524.
11. Y. He, X. Wang, L. Chen and J. D. Ding, *Journal of Materials Chemistry B*, 2014, **2**, 2220-2227.
12. X. Zhang, F. Shi, J. Niu, Y. G. Jiang and Z. Q. Wang, *J. Mater. Chem.*, 2008, **18**, 621-633.
13. X. J. Feng and L. Jiang, *Adv. Mater.*, 2006, **18**, 3063-3078.
14. L. Marcon, A. Addad, Y. Coffinier and R. Boukherroub, *Acta Biomaterialia*, 2013, **9**, 4585-4591.
15. G. Jing, Y. Wang, T. Zhou, S. F. Perry, M. T. Grimes and S. Tatic-Lucic, *Acta Biomaterialia*, 2011, **7**, 1094-1103.
16. Y. H. Lai, J. T. Yang and D. B. Shieh, *Lab on a Chip*, 2010, **10**, 499-504.
17. K. Hecht, N. Schuler, A. Dubbe, M. Kraut, P. Pfeifer and R. Dittmeyer, *Journal of Chemical Engineering of Japan*, 2012, **45**, 727-733.
18. L. Zhang, H. Z. Yu, N. Zhao, Z. M. Dang and J. Xu, *Journal of Applied Polymer Science*, 2014, **131**, 6.
19. Q. M. Yin, J. M. Ye and Y. L. Zhou, *Chem. J. Chin. Univ.-Chin.*, 2008, **29**, 1647-1649.
20. J. El-Ali, P. K. Sorger and K. F. Jensen, *Nature*, 2006, **442**, 403-411.
21. X. Y. Jiang, D. A. Bruzewicz, A. P. Wong, M. Piel and G. M. Whitesides, *Proceedings of the National Academy of Sciences of the United States of America*, 2005, **102**, 975-978.
22. R. Kapur, K. A. Giuliano, M. Campana, T. Adams, K. Olson, D. Jung, M. Mrksich, C. Vasudevan and D. L. Taylor, *Biomedical Microdevices*, 1999, **2**, 99-109.
23. J. Yang, M. Yamato and T. Okano, *MRS Bull.*, 2005, **30**, 189-193.
24. N. M. Alves, J. Shi, E. Oramas, J. L. Santos, H. Tomas and J. F. Mano, *Journal of Biomedical Materials Research Part A*, 2009, **91A**, 480-488.
25. C. Yan, J. G. Sun and J. D. Ding, *Biomaterials*, 2011, **32**, 3931-3938.
26. I. Y. Wong, B. D. Almquist and N. A. Melosh, *Materials Today*, 2010, **13**, 14-22.
27. C. A. Goubko and X. D. Cao, *Mater. Sci. Eng. C-Mater. Biol. Appl.*, 2009, **29**, 1855-1868.
28. J. Shi, N. M. Alves and J. F. Mano, *Bioinspiration & Biomimetics*, 2008, **3**.
29. P. E. Scopelliti, A. Borgonovo, M. Indrieri, L. Giorgetti, G. Bongiorno, R. Carbone, A. Podesta and P. Milani, *Plos One*, 2010, **5**.
30. Y. Ito and M. Nogawa, *Biomaterials*, 2003, **24**, 3021-3026.
31. D. M. Thompson and H. M. Buettner, *Tissue Eng.*, 2001, **7**, 247-265.
32. J. Tang, R. Peng and J. D. Ding, *Biomaterials*, 2010, **31**, 2470-2476.
33. X. T. Shi, L. Li, S. Ostrovidov, Y. W. Shu, A. Khademhosseini and H. K. Wu, *Acs Applied Materials & Interfaces*, 2014, **6**, 11915-11923.
34. F. Yao, H. Hu, S. L. Xu, R. J. Huo, Z. P. Zhao, F. Z. Zhang and F. J. Xu, *Acs Applied Materials & Interfaces*, 2015, **7**, 3882-3887.
35. R. Branemark, L. O. Ohrnell, R. Skalak, L. Carlsson and P. I. Branemark, *J. Orthop. Res.*, 1998, **16**, 61-69.
36. J. E. Davies, *Anatomical Record*, 1996, **245**, 426-445.
37. M. Ysander, R. Branemark, K. Olmarker and R. R. Myers, *Journal of Rehabilitation Research and Development*, 2001, **38**, 183-190.
38. J. E. Davies and N. Baldan, *Journal of Biomedical Materials Research*, 1997, **36**, 429-440.
39. W. J. Weng, S. Zhang, K. Cheng, H. B. Qu, P. Y. Du, G. Shen, J. Yuan and G. R. Han, *Surface & Coatings Technology*, 2003, **167**, 292-296.
40. W. Pompe, H. Worch, W. Habraken, P. Simon, R. Kniep, H. Ehrlich and P. Paufler, *Journal of Materials Chemistry B*,

2015, **3**, 5318-5329.
41. D. Sriranganathan, N. Kanwal, K. A. Hing and R. G. Hill, *Journal of Materials Science-Materials in Medicine*, 2016, **27**.
42. W. E. Brown, N. Eidelman and B. Tomazic, *Advances in dental research*, 1987, **1**, 306-313.
43. M. S. A. Johnsson and G. H. Nancollas, *Critical Reviews in Oral Biology & Medicine*, 1992, **3**, 61-82.
44. P. L. Jiang, J. H. Liang, R. Song, Y. M. Zhang, L. Ren, L. H. Zhang, P. F. Tang and C. J. Lin, *Acs Applied Materials & Interfaces*, 2015, **7**, 14384-14396.
45. Z. Hadisi, J. Nourmohammadi and J. Mohammadi, *Ceramics International*, 2015, **41**, 10745-10754.
46. Y. Liu, R. M. Shelton, U. Gbureck and J. E. Barralet, *Journal of Biomedical Materials Research Part A*, 2009, **90A**, 972-980.
47. M. Yamaguchi, K. Ikeda, M. Suzuki, A. Kiyohara, S. N. Kudoh, K. Shimizu, T. Taira, D. Ito, T. Uchida and K. Gohara, *Langmuir*, 2011, **27**, 12521-12532.
48. A. Shishido, I. B. Divilianskiy, I. C. Khoo, T. S. Mayer, S. Nishimura, G. L. Egan and T. E. Mallouk, *Applied Physics Letters*, 2001, **79**, 3332-3334.
49. J. B. Gan, H. Chen, F. Zhou, H. Huang, J. Zheng, W. Song, L. Yuan and Z. K. Wu, *Colloid Surf. B-Biointerfaces*, 2010, **76**, 381-385.
50. J. Doh and D. J. Irvine, *Journal of the American Chemical Society*, 2004, **126**, 9170-9171.
51. A. Scandurra, G. F. Indelli and S. Pignataro, *Surface and Interface Analysis*, 2012, **44**, 1171-1176.
52. X. M. Zhao, Y. N. Xia and G. M. Whitesides, *J. Mater. Chem.*, 1997, **7**, 1069-1074.
53. S. H. Park and Y. N. Xia, *Chem. Mat.*, 1998, **10**, 1745-+.
54. J. Peng, Y. C. Han, J. Fu, Y. M. Yang and B. Y. Li, *Macromolecular Chemistry and Physics*, 2003, **204**, 125-130.
55. E. Ostuni, C. S. Chen, D. E. Ingber and G. M. Whitesides, *Langmuir*, 2001, **17**, 2828-2834.
56. N. Tanaka, H. Ota, K. Fukumori, J. Miyake, M. Yamato and T. Okano, *Biomaterials*, 2014, **35**, 9802-9810.
57. L. Filipponi, P. Livingston, O. Kaspar, V. Tokarova and D. V. Nicolau, *Biomedical Microdevices*, 2016, **18**.
58. P. Xiao, J. C. Gu, J. Chen, J. W. Zhang, R. B. Xing, Y. C. Han, J. Fu, W. Q. Wang and T. Chen, *Chem. Commun.*, 2014, **50**, 7103-7106.
59. S. Han, S. Hong, H. W. Kang, M. Wanit, B. Kang and S. H. Ko, *Journal of Micromechanics and Microengineering*, 2015, **25**.
60. M. J. Jang and Y. Nam, *Macromolecular Bioscience*, 2015, **15**, 613-621.
61. K. B. Kim, M. S. Kim, D. H. Lee, B. M. Choi, K. S. Jung, S. H. Jung, J. K. Lee, O. Beom-Hoan, S. G. Lee and S. G. Park, *Microelectronic Engineering*, 2015, **145**, 160-165.
62. S. R. Sousa, P. Moradas-Ferreira, B. Saramago, L. V. Melo and M. A. Barbosa, *Langmuir*, 2004, **20**, 9745-9754.
63. W. Han, Y. D. Wang and Y. F. Zheng, in *Multi-Functional Materials and Structures, Pts 1 and 2*, eds. A. K. T. Lau, J. Lu, V. K. Varadan, F. K. Chang, J. P. Tu and P. M. Lam, 2008, vol. 47-50, pp. 1438-1441.
64. D. Chen, Y. F. Gao, G. Wang, H. Zhang, W. Lu and J. H. Li, *Journal of Physical Chemistry C*, 2007, **111**, 13163-13169.
65. O. Carp, C. L. Huisman and A. Reller, *Progress in Solid State Chemistry*, 2004, **32**, 33-177.
66. A. Fujishima, X. T. Zhang and D. A. Tryk, *Surface Science Reports*, 2008, **63**, 515-582.
67. H. Noh, S. G. Oh and S. S. Im, *Applied Surface Science*, 2015, **333**, 157-162.
68. M. K. Nazeeruddin, P. Pechy, T. Renouard, S. M. Zakeeruddin, R. Humphry-Baker, P. Comte, P. Liska, L. Cevey, E. Costa, V. Shklover, L. Spiccia, G. B. Deacon, C. A. Bignozzi and M. Gratzel, *Journal of the American Chemical Society*, 2001, **123**, 1613-1624.
69. J. Y. Lee, C. Jones, M. A. Zern and A. Revzin, *Analytical Chemistry*, 2006, **78**, 8305-8312.
70. R. Zhang, M. Chen, Q. J. Xue, F. Guan and S. Liang, *Chem. J. Chin. Univ.-Chin.*, 2005, **26**, 939-941.
71. K. Nakata, S. Nishimoto, A. Kubo, D. Tryk, T. Ochiai, T. Murakami and A. Fujishima, *Chem.-Asian J.*, 2009, **4**, 984-988.
72. J. T. Park, D. K. Roh, R. Patel, K. J. Son, W. G. Koh and J. H. Kim, *Electrochim. Acta*, 2010, **56**, 68-73.
73. Y. K. Lai, Z. Q. Lin, Z. Chen, J. Y. Huang and C. J. Lin, *Mater. Lett.*, 2010, **64**, 1309-1312.
74. F. Guan, M. Chen, R. Zhang, S. Liang and Q. J. Xue, *Chem. J. Chin. Univ.-Chin.*, 2005, **26**, 599-602.
75. S. Liang, M. Chen, Q. J. Xue, Y. L. Qi and J. M. Chen, *Journal of Colloid and Interface Science*, 2007, **311**, 194-202.
76. G. K. Mor, O. K. Varghese, M. Paulose and C. A. Grimes, *Advanced Functional Materials*, 2005, **15**, 1291-1296.
77. S. Berger, A. Ghicov, Y. C. Nah and P. Schmuki, *Langmuir*, 2009, **25**, 4841-4844.
78. Y. K. Lai, J. Y. Huang, J. J. Gong, Y. X. Huang, C. L. Wang, Z. Chen and C. J. Lin, *Journal of the Electrochemical Society*, 2009, **156**, D480-D484.
79. S. Hiromoto, M. Inoue, T. Taguchi, M. Yamane and N. Ohtsu, *Acta Biomaterialia*, 2015, **11**, 520-530.
80. J. Kunze, L. Muller, J. M. Macak, P. Greil, P. Schmuki and F. A. Muller, *Electrochim. Acta*, 2008, **53**, 6995-7003.
81. T. Ishizaki, N. Saito and O. Takai, *Langmuir*, 2010, **26**, 8147-8154.
82. D. J. Iuliano, S. S. Saavedra and G. A. Truskey, *Journal of Biomedical Materials Research*, 1993, **27**, 1103-1113.
83. J. S. Choi, D. H. Kim and T. S. Seo, *Biomaterials*, 2016, **84**, 315-322.
84. L. C. Boraas, J. B. Guidry, E. T. Pineda and T. Ahsan, *Plos One*, 2016, **11**.
85. S. Lumetti, E. Manfredi, S. Ferraris, S. Spriano, G. Passeri, G. Ghiacci, G. Macaluso and C. Galli, *Journal of Materials Science-Materials in Medicine*, 2016, **27**, 9.
86. H. S. Park, S. Y. Lee, H. Yoon and I. Noh, *Pure and Applied Chemistry*, 2014, **86**, 1911-1922.

Graphical Abstract

A facile construction of gradient micro-patterned OCP coatings on titanium was developed for high-throughput screening of biocompatibility and bioactivity.